Structural Engineering and Mechanics, Vol. 36, No. 4 (2010) 447-461 447
DOI: http://dx.doi.org/10.12989/sem.2010.36.4.447

Effects of tensile softening on the cracking resistance of FRP reinforced concrete under thermal loads

Pattamad Panedpojaman[a] and Thanyawat Pothisiri*

Department of Civil Engineering, Chulalongkorn University, Phayathai Road, Pathumwan, Bangkok 10330, Thailand

(Received March 8, 2010, Accepted July 16, 2010)

Abstract. Fiber reinforced polymer (FRP) bars have been widely used as reinforcement for concrete structures. However, under elevated temperatures, the difference between the transverse coefficients of thermal expansion of FRP rebars and concrete may cause the splitting cracks of the concrete cover. As a result, the bonding of FRP-reinforced concrete may not sustain its function to transfer load between the FRP rebar and the surrounding concrete. The current study investigates the cracking resistance of FRP reinforced concrete against the thermal expansion based on a mechanical model that accounts for the tensile softening behavior of concrete. To evaluate the efficacy of the proposed model, the critical temperature increments at which the splitting failure of the concrete cover occurs and the internal crack radii estimated are compared with the results obtained from the previous studies. Simplified equations for estimating the critical temperature increments and the minimum concrete cover required to prevent concrete splitting failure for a designated temperature increment are also derived for design purpose.

Keywords: thermal expansion; splitting crack; FRP reinforced concrete; tensile softening.

1. Introduction

The composite materials of fiber reinforced polymer (FRP), i.e., fibers (organic or inorganic) and a polymeric resin cause an anisotropic behavior for both mechanical and thermal properties. The longitudinal mechanical properties of FRP bars depend upon the type of fibers while the transverse mechanical properties are determined by the polymeric resin. For the thermal properties, the transverse coefficient of thermal expansion of FRP bars is higher than that of concrete up to eight times whereas the longitudinal coefficient of thermal expansion is approximately zero for Carbon or Aramid-based FRP. For Glass FRP, the longitudinal coefficient of thermal expansion is within the same range as concrete (Abdalla 2006, ACI 2006). Many previous experimental studies (Aiello *et al.* 2001, Masmoudi *et al.* 2005) have shown that due to the different transverse coefficients of thermal expansion of concrete and FRP rebars, the concrete cover of FRP reinforced concrete may split at a certain level of temperature increase, the so-called critical temperature increment. The splitting cracks of the concrete cover affect the bond between the FRP rebars and concrete (Sakai *et al.* 1999, Wang and Liu 2003) which could in turn influence the structural response.

---

*Corresponding author, Associate Professor, E-mail: fcetps@eng.chula.ac.th
[a]Ph.D. Student

The previous investigations on the effects of thermal loads on FRP reinforced concrete have focused on the critical temperature increment that causes internal splitting cracks and the sufficient concrete cover to prevent the splitting failure. Various finite element models (Gentry and Husain 1999, Abdalla 2006) and a mesoscopic thermoelastic damage (MTED) model (Wong *et al.* 2006) have also been proposed to predict the internal damage or the splitting failure patterns of the concrete cover of FRP reinforced elements. These models require proficient skills to solve the problem which may not be convenient for normal use or design. Aiello *et al.* (2001) proposed an analytical model based on the elastic theory of thick-wall cylinders to determine the critical temperature increment corresponding to the initiation of cracking and the sufficient thickness of the concrete cover to prevent the splitting failure of FRP reinforced concrete elements due to the differential thermal expansion of concrete and FRP rebars.

The analysis of the thermal effects can be performed by considering the concrete as a thick-walled cylinder surrounding the FRP rebar in which the differential thermal expansion is regarded as the radial pressure imposed upon the concrete at the FRP bar-concrete interface. The thermal pressure is equilibrated by the pressure resistance of the concrete cover through the induced tensile stresses in the surrounding concrete. When the maximum tensile stress exceeds the tensile strength of the concrete cover, cracking is initiated. After cracking, the pressure can still be transferred through the inner cracked concrete core to the outer sound concrete cover which remains elastic (Sakai *et al.* 1999, Aiello *et al*. 2001, Wang and Liu 2003). The partially cracked concrete cover can sustain the pressure resistance against the induced tensile stresses by considering the softening behavior of the concrete after cracking (Wang and Liu 2003). Based on our preliminary studies, the pressure resistance computed by taking into account the tensile softening behavior of the concrete better agrees with the experimental results (Tepfers 1979, Tepfers and De Lorenzis 2003) for normal-temperature cases. However, previous research works (Tepfers 1979, Sakai *et al.* 1999, Aiello *et al*. 2001) have neglected the softening behavior in computing the pressure resistance of FRP reinforced concrete under thermal loads.

In this paper an analytical model is presented to investigate the effects of tensile softening on the pressure resistance of FRP reinforced concrete under thermal loads. The analysis is performed by adopting the tensile softening model proposed by Wang and Liu (2003) to compute the critical temperature increment and the minimum concrete cover required to prevent the splitting failure. In addition, the internal crack radii of the concrete cover at temperatures lower than the critical temperature increment are also investigated. The results are compared with previous solutions and experimental results (Aiello 1999, Aiello *et al.* 2001, Masmoudi *et al.* 2005, Wong *et al.* 2006, Zaidi and Masmoudi 2008) to determine the extent of softening effects upon the pressure resistance of FRP reinforced concrete.

2. Analytical model

Based on the same methodology as proposed in the literature (Aiello *et al*. 2001, Masmoudi *et al.* 2005), the analytical investigation is carried out considering a cylindrical FRP bar embedded in a concrete cylinder as illustrated in Fig. 1(a) in which the rebar of radius $r_0 = d/2$ is embedded in the concrete with outer radius, r_u, the concrete cover dimension measured from the center of the rebar to the nearest surface of concrete. The cracking resistance of concrete can be determined by considering a radial pressure, p, acting at the surface of the rebar-concrete interface (Fig. 1(b)). Note

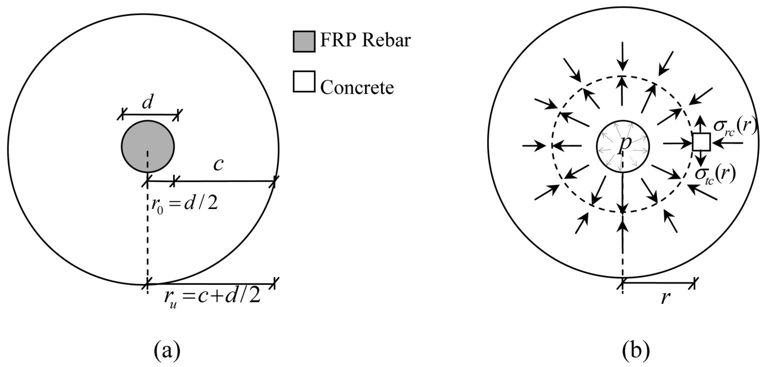

Fig. 1 Modeling of the cracking resistance of FRP reinforced concrete

that the theoretical model presented herein is analyzed based on the following assumptions: 1) effect of transverse reinforcement is neglected in order to evaluate only the pressure resistance of the concrete cover (Tepfers 1979, Sakai *et al.* 1999, Aiello *et al.* 2001, Wang and Liu 2003), 2) FRP bars present a linear elastic behavior (Aiello *et al*. 2001); and 3) cracked concrete presents a tensile softening behavior (Wang and Liu 2003) whereas uncracked concrete sustains its linear elastic behavior.

2.1 Cracking resistance of the concrete cover at normal temperature

For normal-temperature conditions, the model in Fig. 1 can be analyzed as having no temperature increment ($\Delta T = 0$). Prior to the formation of the splitting cracks, the behavior of the concrete cover remains in its elastic stage. The radial pressure p at the internal surface of the cylindrical concrete hole induces the radial compression $\sigma_{rc}(r)$ and the circumferential tension $\sigma_{tc}(r)$ as shown in Fig. 1(b). At a certain radial distance r from the centerline of the rebar, $\sigma_{rc}(r)$ and $\sigma_{tc}(r)$ can be determined by using the theory of elasticity as follows

$$\sigma_{rc}(r) = \frac{r_0^2 p}{r_u^2 - r_0^2}\left(1 - \frac{r_u^2}{r^2}\right) \tag{1}$$

$$\sigma_{tc}(r) = \frac{r_0^2 p}{r_u^2 - r_0^2}\left(1 + \frac{r_u^2}{r^2}\right) \tag{2}$$

The stresses obtained from the above equations can be used only before the tensile stress in the circumferential direction $\sigma_{tc}(r)$ exceeds the tensile strength of the concrete cover f_{tc} (see Fig. 2(a)). At which point, the radial pressure in the elastic stage, p_{ce}, at the interface between the FRP rebar and the surrounding concrete ($r = r_0$) can be obtained by substituting $\sigma_{tc}(r)$ in Eq. (2) with the tensile strength of concrete f_{tc}

$$p_{ce} = f_{tc}\frac{r_u^2 - r_0^2}{r_u^2 + r_0^2} \tag{3}$$

Once the circumferential tension at the FRP rebar-concrete interface, $\sigma_{tc}(r_0)$, exceeds the tensile strength of concrete, the splitting cracks take place. After cracking, the surrounding concrete

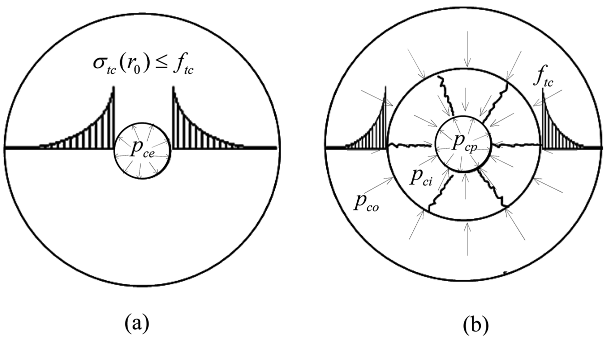

Fig. 2 (a) distribution of tensile ring stresses in the elastic stage, (b) distribution of tensile ring stresses in the partially cracked elastic stage (Tepfers 1982)

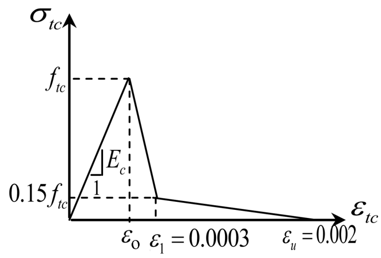

Fig. 3 Stress-strain relationship for concrete in tension (Pantazopoulou 2001)

cylinder can be divided into two zones (see Fig. 2(b)). The concrete within the outer zone does not crack and sustains its elastic behavior whereas the concrete is considered cracked throughout the inner zone. The boundary of the inner zone can be specified by the distance at which the splitting cracks propagate to, the so-called inner crack radius r_l. Based on the softening model of Wang and Liu (2003), the relationship between the tensile stress ($\sigma_{tc}(r)$) and the tensile strain ($\varepsilon_{tc}(r)$) of cracked concrete can be regarded as a process of softening once the tensile strain of concrete $\varepsilon_{tc}(r)$ exceeds the elastic limit ε_0 as illustrated in Fig. 3 (Pantazopoulou and Papoulia 2001) in which E_c is the initial elastic modulus of concrete. Consequently, the radial pressure of concrete in the partially cracked elastic stage, p_{cp}, can be computed as the sum of the resisting pressure of concrete in the outer zone p_{co} and the resisting pressure of concrete in the inner zone p_{ci} by using the following pressure equilibrium equation.

$$2\pi r_0 p_{cp} = 2\pi r_i p_{co} + 2\pi r_0 p_{ci} \tag{4}$$

or

$$p_{cp} = \left(\frac{r_i}{r_0}\right) p_{co} + p_{ci} \tag{5}$$

whereas the resisting pressure of concrete in the outer zone p_{co} which is in the elastic stage can be obtained by substituting the term r_0 in Eq. (3) with r_i

$$p_{co} = f_{tc}\left(\frac{r_u^2 - (r_i)^2}{r_u^2 + (r_i)^2}\right) \tag{6}$$

The resisting pressure of concrete in the inner zone p_{ci} which is in the cracked stage can be computed by integrating the circumferential stress $\sigma_{tc}(r)$ over the cracked inner part

$$p_{ci} = \frac{1}{r_0}\int_{r_0}^{r_i} \sigma_{tc}(r)dr \tag{7}$$

Based on Wang and Liu (2003), the circumferential tension $\sigma_{tc}(r)$ in the cracked concrete zone can be computed by neglecting the Poisson's effect and assuming that the radial displacement $u_{rc}(r)$ associated with the tensile strain $\varepsilon_{tc}(r)$ is constant throughout the cracked part and equal to the radial displacement at the inner radius, u_{r_i}:

$$u_{rc}(r) = r\varepsilon_{tc}(r) = u_{r_i} = r_i\varepsilon_0 \tag{8}$$

or

$$\varepsilon_{tc}(r) = \frac{r_i}{r}\varepsilon_0 \tag{9}$$

The tensile strain of the cracked concrete in Eq. (9) can be converted to the tensile stress using the stress-strain relationship of Fig. 3 in which the integral in Eq. (7) can be solved (Wang and Liu 2003):

$$\int_{r_0}^{r_i} \sigma_{tc}(r)dr = \frac{f_{tc}}{\varepsilon_1 - \varepsilon_0}\left[(\varepsilon_1 - 0.15\varepsilon_0)(r_i - r_0) - 0.85 r_i\varepsilon_0 \ln\frac{r_i}{r_0}\right] \quad \text{for} \quad \frac{r_i}{r_0} < \frac{r_u}{r_0} \le \frac{\varepsilon_1}{\varepsilon_0} \tag{10-1}$$

$$\int_{r_0}^{r_i} \sigma_{tc}(r)dr = I_1 + I_2 \quad \text{for} \quad \frac{\varepsilon_1}{\varepsilon_0} < \frac{r_i}{r_0} < \frac{r_u}{r_0} \le \frac{\varepsilon_u}{\varepsilon_0} \tag{10-2}$$

where

$$I_1 = \int_{r_0}^{r_1} \sigma_{tc}(r)dr = \frac{0.15 f_{tc}}{\varepsilon_u - \varepsilon_1}\left[\varepsilon_u \frac{r_i\varepsilon_0 - r_0\varepsilon_1}{\varepsilon_1} - r_i\varepsilon_0 \ln\frac{r_i\varepsilon_0}{r_0\varepsilon_1}\right]$$

$$I_2 = \int_{r_1}^{r_i} \sigma_{tc}(r)dr = \frac{f_{tc}}{\varepsilon_1 - \varepsilon_0}\left[(\varepsilon_1 - 0.15\varepsilon_0) r_i \frac{(\varepsilon_1 - \varepsilon_0)}{\varepsilon_1} - 0.85 r_i\varepsilon_0 \ln\frac{\varepsilon_1}{\varepsilon_0}\right]$$

with $r_1 = \dfrac{r_i\varepsilon_0}{\varepsilon_1}$

The radial pressure of concrete in the partially cracked elastic stage p_{cp} can be obtained by substituting Eqs. (7), (10-1) and (10-2) into Eq. (5). The maximum value of the radial pressure $p_{cp,\max}$ can be computed by differentiating p_{cp} in Eq. (5) with respect to r_i and set to zero:

$$\frac{dp_{cp}}{dr_i} = \left(\frac{r_u^4 - r_i^4 - 4r_i^4 r_u^4}{r_0(r_u^2 - r_i^2)^2}\right) f_{tc} + \frac{dp_{ci}}{dr_i} = 0 \tag{11}$$

where

$$\frac{dp_{ci}}{dr_i} = \frac{f_{tc}}{(\varepsilon_1 - \varepsilon_0)r_0}\left[(\varepsilon_1 - 0.15\varepsilon_0) - 0.85\varepsilon_0\left(1 + \ln\frac{r_i}{r_0}\right)\right] \quad \text{for} \quad \frac{r_i}{r_0} < \frac{r_u}{r_0} \le \frac{\varepsilon_1}{\varepsilon_0}$$

$$\frac{dp_{ci}}{dr_i} = \frac{0.15 f_{tc}}{(\varepsilon_2 - \varepsilon_1)r_0}\left[\frac{\varepsilon_0\varepsilon_2}{\varepsilon_1} - \varepsilon_0\left(1 + \ln\frac{r_i\varepsilon_0}{r_0\varepsilon_1}\right)\right] + \frac{f_{tc}}{r_0}\left[\frac{(\varepsilon_1 - 0.15\varepsilon_0)}{\varepsilon_1} - \frac{0.85\varepsilon_0}{(\varepsilon_1 - \varepsilon_0)}\ln\frac{\varepsilon_1}{\varepsilon_0}\right]$$

$$\text{for} \quad \frac{\varepsilon_1}{\varepsilon_0} < \frac{r_i}{r_0} < \frac{r_u}{r_0} \le \frac{\varepsilon_u}{\varepsilon_0}$$

The above equation can be solved numerically for r_i which is referred to as the maximum crack radius, $r_{i,\max}$ and the corresponding $p_{cp,\max}$ is taken as the cracking resistance of the concrete.

2.2 Cracking resistance of the concrete cover at elevated temperatures

At elevated temperatures, the FRP reinforced concrete model in Fig. 1 can be considered to be subjected to a temperature increment ΔT. The differential thermal expansion of the FRP rebar and the surrounding concrete causes additional radial pressure against the internal surface of the concrete cylinder. When the temperature increment ΔT is low, the behavior of concrete can be considered to be in the elastic stage as long as the induced circumferential strain of concrete at the rebar-concrete interface $\varepsilon_{tc,\Delta T}(r_0)$, is below the elastic tensile strain limit ε_0. The relationship between the tensile strain of concrete $\varepsilon_{tc,\Delta T}(r_0)$ and the radial pressure of concrete $p_{ce,\Delta T}$ at the rebar-concrete interface can then be derived as (Rahman *et al.* 1995, Aiello *et al.* 2001):

$$\varepsilon_{tc,\Delta T}(r_0) = \frac{p_{ce,\Delta T}}{E_c}\left(\frac{r_u^2 + r_0^2}{r_u^2 - r_0^2} + \nu_c\right) + \alpha_c \Delta T \tag{12}$$

whereas the elastic tensile strain of the FRP rebar $\varepsilon_{tb,\Delta T}$ at the rebar-concrete interface can be computed as:

$$\varepsilon_{tb,\Delta T}(r_0) = \alpha_b \Delta T - \frac{p_{ce,\Delta T}(1-\nu_b)}{E_b} \tag{13}$$

in which

α_c and α_b are the transverse thermal coefficients of expansion of the concrete and the FRP rebar;
ν_c is the Poisson's ratio of the concrete;
ν_b is the Poisson's ratio of the FRP rebar in the transverse direction; and
E_b is the elastic modulus of the FRP rebar.

Based on the compatibility of the circumferential strains at the rebar-concrete interface (i.e., $\varepsilon_{tb,\Delta T}(r_0) = \varepsilon_{tc,\Delta T}(r_0)$), the radial pressure $p_{ce,\Delta T}$ can be computed by equating Eq. (12) and Eq. (13) as:

$$p_{ce,\Delta T} = \frac{(\alpha_b - \alpha_c)\Delta T}{\frac{1}{E_c}\left(\frac{r_u^2 + r_0^2}{r_u^2 - r_0^2} + \nu_c\right) + \frac{1}{E_b}(1-\nu_b)} \tag{14}$$

Under the increasing temperature increment ΔT, the circumferential strain of concrete may exceed the elastic strain limit ε_0 in which case the concrete can no longer be assumed to behave elastically. The FRP rebar, however, can still be considered to present a linear elastic behavior (Aiello *et al.* 2001). The circumferential strain of the partially cracked concrete cylinder at the rebar-concrete interface subjected to the temperature increment ΔT can be computed as the sum of the tensile strain of concrete within the cracked inner part obtained by Eq. (9) and the thermal expansion of concrete due to ΔT:

$$\varepsilon_{tc,\Delta T}(r_0) = \frac{r_i}{r_0}\varepsilon_0 + \alpha_c \Delta T \tag{15}$$

The compatibility of the circumferential strains at the rebar-concrete interface is obtained by adopting the elastic tensile strain of the FRP rebar in Eq. (13):

$$\frac{r_i}{r_0}\varepsilon_0 + \alpha_c \Delta T = \alpha_b \Delta T - \frac{p_{cp,\Delta T}(1-\nu_b)}{E_b} \tag{16}$$

The radial pressure of the partially cracked concrete under thermal loads, $p_{cp,\Delta T}$, in the above equation can be computed by using Eq. (5) for the range of the temperature increments considered

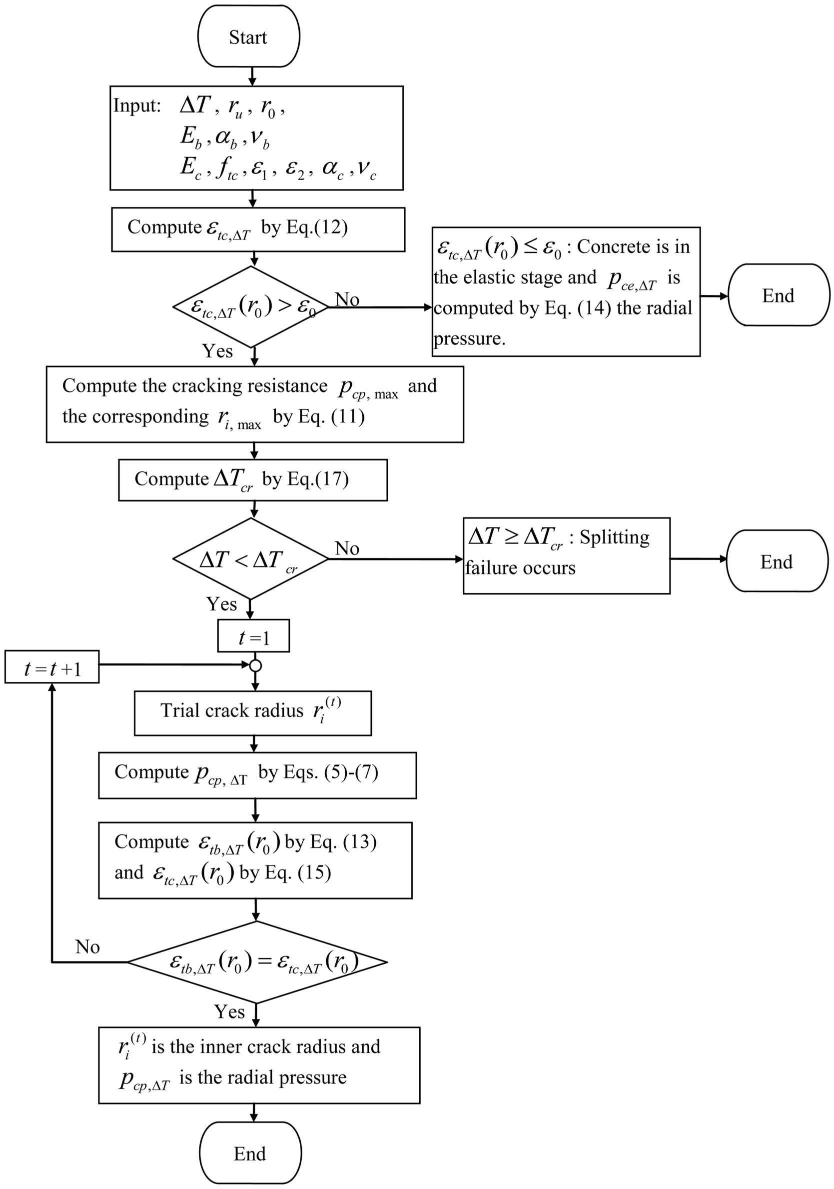

Fig. 4 The computational procedure for the inner crack radius r_i and the radial pressure of concrete $p_{cp,\Delta T}$ for a specified temperature increment ΔT

in this paper ($\Delta T < 100^{\text{o}}\text{C}$) because the properties of concrete are the same as for the normal-temperature case. Whilst, in general cases, the properties of concrete can simply be modified in accordance with the varying temperature increments. Because $p_{cp,\Delta T}$ is a function of the inner crack radius r_i, the solution to Eq. (16) can be obtained numerically for radial pressure $p_{cp,\Delta T}$ by trialing for the value of r_i that satisfies the compatibility condition of Eq. (16).

When the temperature increment ΔT reaches a specific value at which the radial pressure $p_{cp,\Delta T}$ obtained from Eq. (16) is equal to the cracking resistance of concrete $p_{cp,\max}$ as determined by Eq. (11), the splitting failure takes place. The temperature increment ΔT at which $p_{cp,\Delta T} = p_{cp,\max}$ is denoted as the critical temperature increment ΔT_{cr}. By substituting the cracking resistance $p_{cp,\max}$ and the corresponding crack radius $r_{i,\max}$ for $p_{cp,\Delta T}$ and r_i in Eq. (16), respectively, the critical temperature increment ΔT_{cr} can be obtained:

$$\Delta T_{cr} = \frac{1}{(\alpha_b - \alpha_c)}\left(\frac{r_{i,\max}}{r_0}\varepsilon_0 + \frac{p_{cp,\max}(1-\nu_b)}{E_b}\right) \tag{17}$$

The procedure to compute the radial pressure of concrete in the elastic stage and the partially cracked elastic stage for a given temperature increment ΔT can be summarized as illustrated in Fig. 4. Note that the cracking resistance $p_{cp,\max}$ of the FRP reinforced concrete model and the corresponding value of the inner crack radius $r_{i,\max}$ can be directly obtained from Eq. (11) after which the critical temperature increment ΔT_{cr} can be computed using Eq. (17).

3. Comparison with previous solutions and experimental results

The critical temperature increment ΔT_{cr} values computed by the proposed model are compared with the results obtained from the previous experiments (Aiello 1999, Aiello *et al.* 2001, Masmoudi *et al.* 2005, Zaidi and Masmoudi 2008), the analytical model of Aiello *et al.* (2001) and the mesoscopic thermoelastic damage (MTED) model of Wong *et al.* (2006) as summarized in Table 1. Note that the previous experimental investigations were conducted for cylindrical and rectangular concrete specimens reinforced with AFRP and GFRP bars which were slowly heated until the splitting failure of concrete occurred. For the rectangular FRP reinforced concrete specimens, the value of c in Table 1 is taken as a shorter distance between one-half of the reinforcement spacing and the minimum concrete cover.

The values of ΔT_{cr} shown in Table 1 are also plotted for different values of *c/d* in Fig. 5. It is seen from Fig. 5 that the proposed model can predict the critical temperature increments values close to the results obtained by the previous experiments and Aiello *et al.*'s model.

The inner crack radius r_i values estimated by the proposed method for FRP reinforced concrete prior to the splitting failure are also compared with the results obtained by the MTED model. Note that because it is difficult, if not virtually impossible, to measure the internal crack radii within concrete specimens, currently there are no experimental data available. The cracking patterns of the concrete cover for a cylindrical FRP reinforced concrete specimen with *c/d* = 4.38 predicted by the MTED model are compared with the crack radii computed by the proposed model as illustrated in Fig. 6. It is apparent from the illustration that the computed crack radii closely approximate the MTED modeling results for the temperature increments ranging between 34ºC-74ºC. However, the proposed model overestimates the critical temperature increment ΔT_{cr} at 85ºC, compared with 76ºC as predicted by the MTED model.

Table 1 Comparison of the ΔT_{cr} values computed by the proposed method with the results obtained from the previous studies

Specimen Geometry	FRP Material Properties	Concrete Material Properties	c/d	Diameter of Rebar (mm)	Critical temperature increment (ºC): Experimental Results	Critical temperature increment (ºC): Aiello *et al.*'s model (2001)	Critical temperature increment (ºC): MTED model (Wong *et al.* 2006)	Critical temperature increment (ºC): Proposed model	References for experimental results
Rectangular	AFRP type $E_b = 3{,}200$ MPa $\nu_b = 0.38$* $\alpha_b = 60.0\times10^{-6}$/ºC	$E_c = 24{,}300$ MPa $f_{tc} = 2.36$ MPa $\nu_c = 0.18$* $\alpha_c = 10.0\times10^{-6}$/ºC	1.19	10	40	14	-	22	Aiello (1999)
			1.25	10	42	14	-	23	
			1.67	10	43	18	-	28	
			2.27	10	43	24	-	37	
		$E_c = 34{,}000$ MPa $f_{tc} = 3.71$ MPa $\nu_c = 0.18$* $\alpha_c = 10.0\times10^{-6}$/ºC	1.00	10	35	17	-	27	
			2.00	10	50	30	-	48	
	GFRP type $E_b = 7{,}100$ MPa $\nu_b = 0.34$ $\alpha_b = 41.2\times10^{-6}$/ºC**	$E_c = 28{,}000$ MPa $f_{tc} = 4.20$ MPa $\nu_c = 0.17$ $\alpha_c = 11.6\times10^{-6}$/ºC	1.00	25	30	22	-	29	Zaidi and Masmoudi (2008)
			1.30	25	40	27	-	35	
			1.40	19	40	29	-	37	
			1.60	16	>60	32	-	41	
			1.80	19,25	>60	36	-	45	
			2.20	16,19,25	>60	44	-	54	
	GFRP type $E_b = 4000$ MPa $\nu_b = 0.40$ $\alpha_b = 58.0\times10^{-6}$/ºC	$E_c = 30{,}000$ MPa $f_{tc} = 3.90$ MPa $\nu_c = 0.18$ $\alpha_c = 12.1\times10^{-6}$/ºC	1.00	13	-	17	36,42,46***	25	Wong *et al.* (2006)
			1.27	13	-	21	28***	30	
			2.00	13	-	30	54,52***	43	
			1.46	13	41	23	-	33	Aiello *et al.* (2001) and Wong *et al.* (2006)
Cylindrical	GFRP type $E_b = 4000$ MPa $\nu_b = 0.40$ $\alpha_b = 58.0\times10^{-6}$/ºC	$E_c = 30{,}000$ MPa $f_{tc} = 3.90$ MPa $\nu_c = 0.18$ $\alpha_c = 12.1\times10^{-6}$/ºC	1.46	13	28	23	35	33	
			2.92	13	70	43	55	60	
			4.38	13	65	65	76	85	
	GFRP type $E_b = 7100$ MPa $\nu_b = 0.38$ $\alpha_b = 31.0\times10^{-6}$/ºC** for $d = 13$ mm $\alpha_b = 34.9\times10^{-6}$/ºC** for $d = 16$ mm $\alpha_b = 36.6\times10^{-6}$/ºC** for $d = 19$ mm $\alpha_b = 43.1\times10^{-6}$/ºC** for $d = 25$ mm	$E_c = 28{,}000$ MPa $f_{tc} = 4.10$ MPa $\nu_c = 0.17$ $\alpha_c = 11.6\times10^{-6}$/ºC	0.80	25	30	16	-	23	Masmoudi *et al.* (2005)
			1.00	25	30	19	-	26	
			1.20	19	30	28	-	36	
			1.50	13,16, 19,25	34.5****	35****	-	44****	

Note: *General properties, **Temperature range: 30ºC to 60ºC, ***The different values of ΔT_{cr} reported for the MTED model are due to the varying configurations of the model, *****Average values.

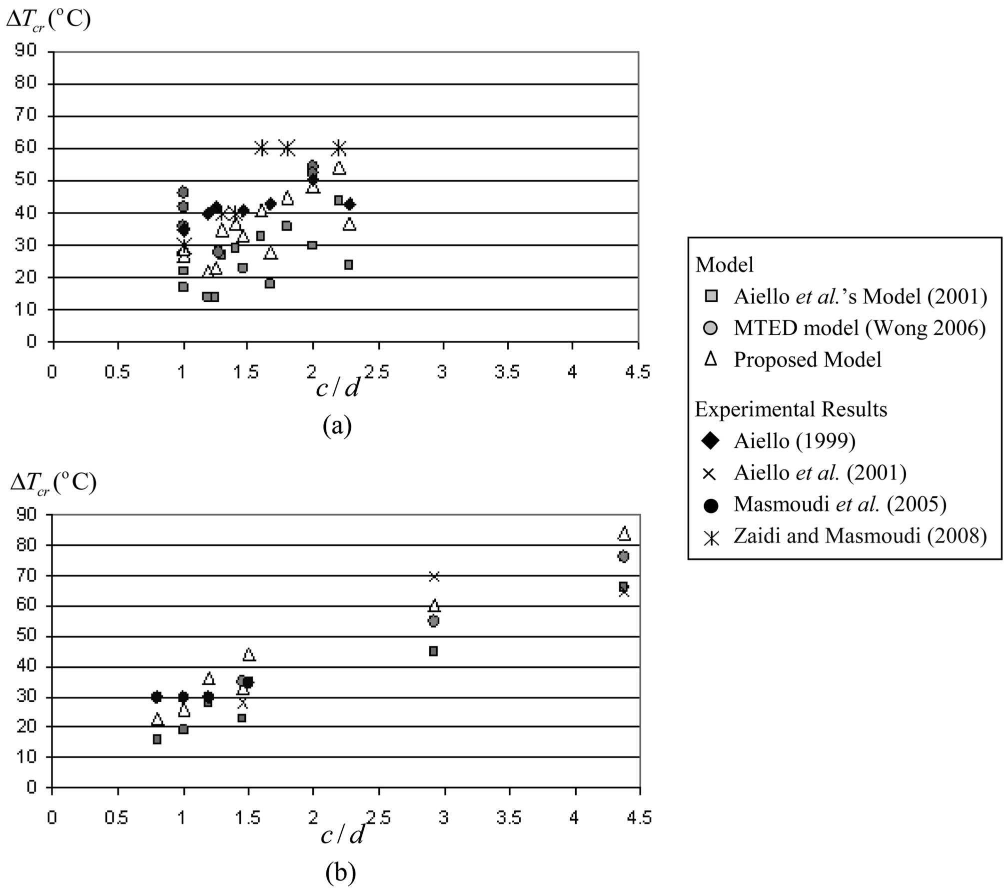

Fig. 5 Variation of ΔT_{cr} with respect to different c/d values for the proposed model compared with the references (a) rectangular specimens and (b) cylindrical specimens

Table 2 Comparison of $p_{cp,\max}$ and $r_{i,\max}$ obtained from the proposed model (with tensile softening) and the Aiello *et al.*'s model (without tensile softening)

c/d	$r_{i,\max}/r_u$		$p_{cp,\max}/f_{tc}$	
	With tensile softening	Without tensile softening	With tensile softening	Without tensile softening
0.20	0.86	N/A	0.38	N/A
0.50	0.81	N/A	0.87	N/A
0.75	0.75	0.48	1.23	0.75
1.00	0.72	0.48	1.57	0.90
1.50	0.68	0.48	2.17	1.20
2.00	0.67	0.48	2.75	1.50
3.00	0.67	0.48	3.90	2.10
4.00	0.67	0.48	5.05	2.71

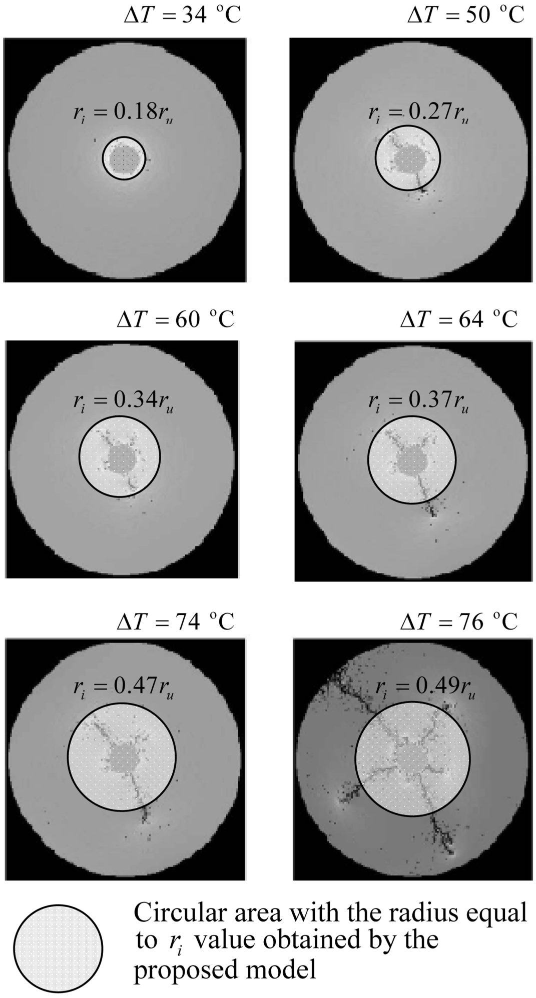

Fig. 6 Comparison between the cracking patterns of the cylindrical FRP reinforced concrete specimens with c/d = 4.38 as predicted by the MTED model and the crack radius r_i values obtained by the proposed model

It can be seen from Table 1 and Fig. 5 that the values of the critical temperature increment ΔT_{cr} obtained from the proposed model are generally higher than those predicted by the Aiello *et al.*'s model due to the tensile softening effect. By incorporating the tensile softening behavior of concrete in the partially cracked elastic stage, the higher values of cracking resistance $p_{cp,\max}$ and the corresponding crack radius $r_{i,\max}$ are obtained. Table 2 provides a comparison between the values of $p_{cp,\max}$ and $r_{i,\max}$ obtained by the proposed model (with tensile softening) and the Aiello *et al.*'s model (without tensile softening) by assuming the relationship $E_c = 8460 f_{tc}$ according to ACI (2005). The results in Table 2 are also plotted in Fig. 7, showing higher values of the cracking resistance $p_{cp,\max}$ for concrete with tensile softening within the range of c/d values considered. It is seen from Table 2 that a constant value of $r_{i,\max} = 0.48r_u$ is obtained from the model without the tensile softening behavior of concrete whereas the values of $r_{i,\max}$ estimated by the proposed model vary

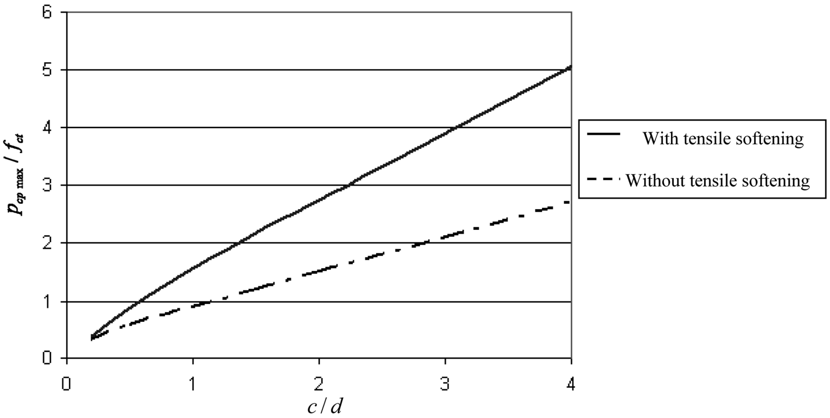

Fig. 7 Variation of the cracking resistance of concrete with and without tensile softening with respect to different c/d values

but converge to $r_{i\,max} = 0.67r_u$. This corresponds with the results of the MTED model (Fu *et al.* 2004 and Wong *et al.* 2006) in which the internal crack radii generally extend longer than $0.60r_u$.

4. Simplified design equations

Based on the proposed procedure, the critical temperature increment ΔT_{cr} can be computed by substituting the cracking resistance $p_{cp,\max}$ and the corresponding crack radius $r_{i,\max}$ into Eq. (17). However, the values of $p_{cp,\max}$ and $r_{i,\max}$ must be obtained through solving Eq. (11) numerically which may not be convenient for design purpose. Therefore, we propose simplified equations for estimating $r_{i,\max}$ and $p_{cp,\max}$ through a linear regression analysis of the values of the normalized crack radius ($r_{i,\max}/r_0$) and the normalized cracking resistance ($p_{cp,\max}/f_{tc}$) that are obtained from the proposed model for a range of c/d values as shown in Fig. 8:

$$r_{i,\max}/r_0 = 1.27c/d + 0.89 \quad \text{with} \quad R^2 = 0.995 \tag{18}$$

$$p_{cp,\max}/f_{tc} = 1.20c/d + 0.31 \quad \text{with} \quad R^2 = 0.988 \tag{19}$$

in which R^2 is the coefficient of determination. Note that the above equations are derived by assuming the relationship $E_c = 8460f_{tc}$ according to ACI (2005). By substituting the simplified equations for $r_{i,\max}/r_0$ and $p_{cp,\max}/f_{tc}$ and the relationship $E_c = 8460f_{tc}$ into Eq. (17), we obtain the simplified equation for critical temperature increment ΔT_{cr} as:

$$\Delta T_{cr} = \frac{1}{(\alpha_b - \alpha_c)}\left(\frac{1.27c/d + 0.89}{8460} + \frac{(1.20c/d + 0.31)f_{tc}(1 - \nu_b)}{E_b}\right) \tag{20}$$

Since the above equation is derived by using the relationship between E_c and f_{tc} in accordance with ACI (2005), the variation of this relationship (i.e., E_c/f_{tc} ratios) must be examined in the calculation of ΔT_{cr} by Eq. (20). The material properties for GFRP rebar and concrete with varying E_c with respect to the same value of f_{tc} in Table 3 are used to compute ΔT_{cr} for the specified range of c/d values based on the procedure in Fig. 4. The results are then compared with the ΔT_{cr} values

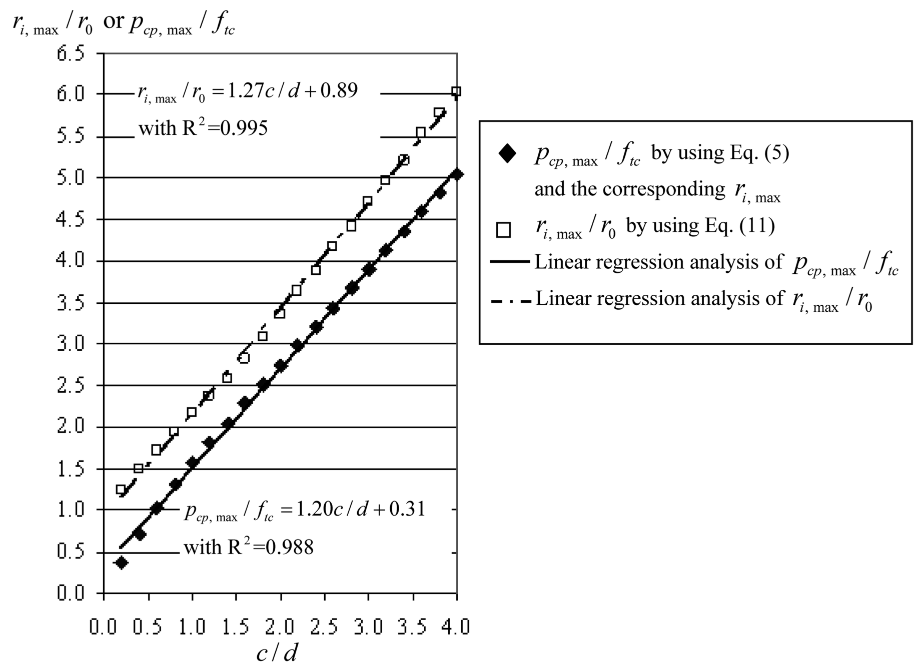

Fig. 8 Linear regression of $r_{i,\max}/r_0$ and $p_{cp,\max}/f_{ct}$ with respect to c/d

Table 3 Material properties for ΔT_{cr} trial calculations

Material properties					
Concrete	f_{tc}	4.2 MPa	GFRP bar	E_b	7,100 MPa
	E_c (E_c/f_{tc})	28,000 MPa (6,700) 35,000 MPa (8,300) 42,000 MPa (10,000)			
	α_c	11.6×10^{-6}/°C		α_b	41.2×10^{-6}/°C
	ν_c	0.17		ν_b	0.34

estimated by using Eq. (20) as illustrated in Fig. 9. From the illustration, we observe good agreements between the ΔT_{cr} values obtained from Eq. (20), which assumes $E_c = 8460 f_{tc}$, and those computed by using the procedure in Fig. 4 with different values of E_c/f_{tc}.

For design purpose, the minimum value of c/d to prevent the splitting failure in a FRP-reinforced concrete element due to a designated temperature increment ΔT_{des} can be obtained by substituting ΔT_{cr} in Eq. (20) with ΔT_{des} and rearranging terms:

$$c/d = \frac{\Delta T_{des}(\alpha_b - \alpha_c) - 6.64 \times 10^{-5}}{15.01 \times 10^{-5} + \dfrac{1.20 f_{tc}(1 - \nu_b)}{E_b}} - 0.26 \tag{21}$$

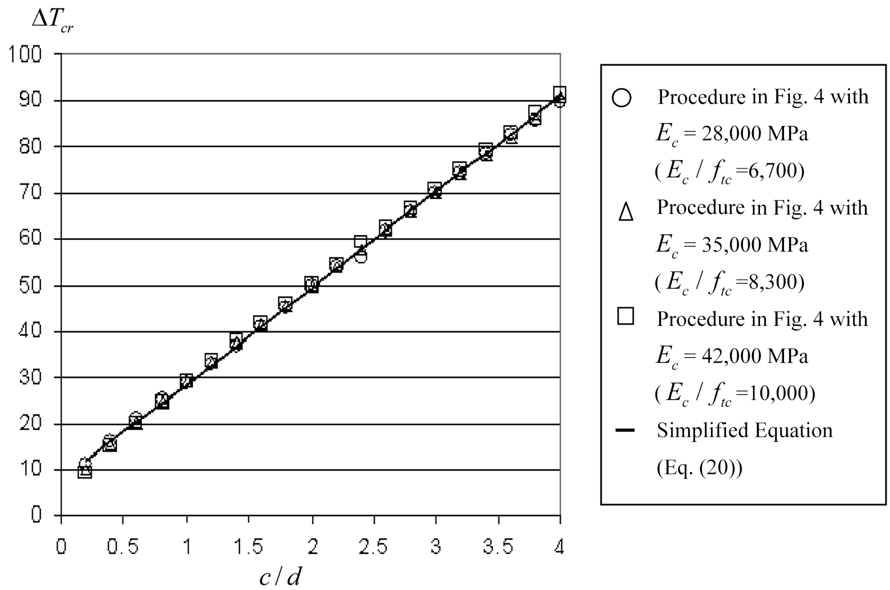

Fig. 9 Comparison of ΔT_{cr} values obtained from the simplified equation and the procedure in Fig. 4

It should, however, be noted that to design the optimal concrete cover for the FRP-reinforced concrete element to prevent the splitting failure, an engineer must also consider the bonding effect (ACI 2005) in addition to the effect of the designated temperature increment ΔT_{des}. The combined effect should be further investigated from the theoretical and experimental point of view. Extensive experimental investigations would allow a correct assessment of the concrete cover to prevent the splitting failure due to the temperature increment and the bonding.

5. Conclusions

An analytical model has been proposed to evaluate the cracking resistance of FRP-reinforced concrete elements under thermal loads taking into account the tensile softening behavior of the partially cracked concrete. It is shown that the maximum crack radii and the cracking resistance of the concrete cover can be increased by the effect of tensile softening, thereby increasing the critical temperature increments for the FRP reinforced concrete. Through comparison with previous solutions and experimental results, it is seen that most of the results obtained from the proposed model agree better with the experimental data for the range of the *c/d* values considered compared with the model without the tensile softening effect. Furthermore, the estimated crack radii at different temperature increments conform with the cracking patterns predicted by the MTED model. It can be implied from the current study that the present model that incorporates the tensile softening effect can better characterize the actual behavior of the partially cracked concrete in evaluating the cracking resistance of FRP reinforced concrete under thermal loads. Finally, through a linear regression analysis we have derived simplified equations for estimating the maximum crack radii, the critical temperature increments and the minimum concrete cover required to prevent the splitting failure, which can be useful for design purpose.

References

Abdalla, H. (2006), "Concrete cover requirements for FRP reinforced members in hot climates", *Compos. Struct.*, **73**, 61-69.

Aiello, M.A. (1999), "Concrete cover failure in FRP reinforced beams under thermal loads", *J. Compos. Construct.*, **3**(1), 46-52.

Aiello, M.A., Focacci, F. and Nanni, A. (2001), "Effects of thermal loads on concrete cover of fiber reinforced polymer reinforced elements: Theoretical and experimental analysis", *ACI Mater. J.*, **98**(4), 332-339.

American Concrete Institute (ACI) (2005), "Building code requirements for structural concrete", 318-05, Detroit.

American Concrete Institute (ACI) (2006), "Guide for the design and construction of concrete with FRP bars", 440.1R-06, Detroit.

Fu, Y.F., Wong, Y.L., Tang, C.A. and Poon, C.S. (2004), "Thermal induced stress and associated cracking in cement-based composite at elevated temperatures—Part II: Thermal cracking around multiple inclusions", *Cement Concrete Compos.*, **26**, 113-126.

Gentry, T.R. and Husain, M. (1999), "Thermal compatibility of concrete and composite reinforcements", *J. Compos. Constr.*, **3**(2), 82-86.

Masmoudi, R., Zaidi, A. and Gérard, P. (2005), "Transverse thermal expansion of FRP bars embedded in Concrete", *J. Compos. Constr.*, **9**(5), 377-387.

Pantazopoulou, S.J. and Papoulia, K.D. (2001), "Modeling cover-cracking due to reinforcement corrosion in RC structures", *J. Eng. Mech.*, **127**(4), 342-351.

Rahman, H.A., Kingsley, C.Y. and Taylor, D.A. (1995), "Thermal stress in FRP reinforced concrete", *Proceedings of the Annual Conference of the Canadian Society for Civil Engineering*, Ottawa, June.

Sakai, T., Kanakubo, T., Yonemaru, K. and Fukuyama, H. (1999), "Bond splitting behavior of continuous fiber reinforced concrete members", *Proceedings of the International Symposium on Fiber-reinforced Polymer for Reinforced Concrete Structures*, Baltimore, MD, ACI SP-188.

Tepfers, R. (1979), "Cracking of concrete cover along anchored deformed reinforcing bars", *Mag. Concrete Res.*, **31**(106), 3-12.

Tepfers, R. (1982), "Lapped tensile reinforcement splices", *J. Struct. Div.-ASCE*, **108**(1), 283-301.

Tepfers, R. and De Lorenzis, L. (2003), "Bond of FRP reinforcement in concrete- a challenge", *Mech. Compos. Mater.,* **39**(4), 315-328.

Wang, X. and Liu, X. (2003), "A tensile-softening model for steel-concrete bond", *Cement. Concrete Res.,* **33**, 1669-1673.

Wong, Y.L., Fu, Y.F., Poon, C.S. and Tang, C.A. (2006), "Spalling of concrete cover of fiber-reinforced polymer reinforced concrete under thermal loads", *Mater. Struct.*, **39**, 991-999.

Zaidi, A. and Masmoudi, R. (2008), "Thermal effect on fiber reinforced polymer reinforced concrete slabs", *Can. J. Civil Eng.*, **35**, 312-320.